Title: Long range correlations of the ion current in SV channels. Met3PbCl influence study

Author: Janusz Miśkiewicz, Zenon Trela, Zbigniew Burdach, Waldemar Karcz, Wanda Balińska-Miśkiewicz
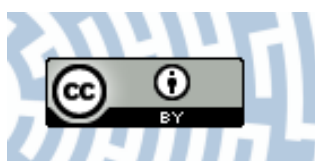
UNIWERSYTET ŚLĄSKI W KATOWICACH   Biblioteka Uniwersytetu Śląskiego   Ministerstwo Nauki i Szkolnictwa Wyższego

RESEARCH ARTICLE

Long range correlations of the ion current in SV channels. Met$_3$PbCl influence study

Janusz Miśkiewicz[1,2]*, **Zenon Trela**[2], **Zbigniew Burdach**[3], **Waldemar Karcz**[3], **Wanda Balińska-Miśkiewicz**[4]

1 Institute of Theoretical Physics, University of Wrocław, Wrocław, Poland, 2 Department of Physics and Biophysics, Wrocław University of Environmental and Life Sciences, Wrocław, Poland, 3 Department of Plant Physiology, Faculty of Biology and Environmental Protection, University of Silesia, Katowice, Poland, 4 1st Department and Clinic of Paediatrics, Allergology and Cardiology, Wroclaw Medical University, Wrocław, Poland

* janusz.miskiewicz@upwr.edu.pl
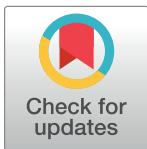
Abstract

The long-range correlations within the current signal time series of the Beta vulgaris vacuolar membrane under the influence of organolead compound (Met$_3$PbCl) are investigated. The current time series is transformed into a dwell time series. Then the rescaled range and detrended fluctuations analyses are used. It is shown that the presence of Met$_3$PbCl in the solution decreases the mean value of the Hurst exponent and therefore influences the long-range correlations in ionic channel current. This observation is statistically significant. An ion channel model is built and the experimental results reconstructed and analysed.

Introduction

This paper is the continuation of the researches on the ionic current influenced by organolead compounds [1]. The previous analysis was focused on the changes of the ion current distribution function related to the Met$_3$PbCl presence while in the present study the correlations in the dwell-time series of the ion channels are investigated. The main aim of the research is to better understand the influence of organolead compounds on the living organisms. It is important to stress that lead is mainly toxic to living organisms, which was reported in various publications e.g. [2–11]. Lead was reported as being the second most hazardous substance, after arsenic, based on the frequency of occurrence, toxicity, and the potential for human exposure by the Agency for Toxic Substances and Disease Registry [12]. Both acute and chronic lead exposure has the potential to cause many serious systematic effects in people including hypertension, anaemia, immune imbalances, infertility, cognitive deficits, adverse effects on nervous and renal systems, delayed skeletal and deciduous dental development, vitamin D deficiency, and gastrointestinal effects [13]. The accepted consensus is that any level of lead is unhealthy [14]. In developing countries, pregnant women and children are still commonly experiencing today the lead concentration in blood in the range 100–500 μg/L when values <50μg/L are desirable [15]. An important source of lead for humans are plants as the food ingredient [16]. The lead toxicity is reported not only in the human aspects but also in plants. Studies on lead

toxicity that have been published in the past decades suggest three main mechanisms of toxicity of Pb^{2+}: inhibition of photosynthesis, oxidative stress, and "genotoxicity" including DNA damage and defects in mitosis [17].

Despite the general understanding of the problem and some successes in lead elimination [18] or even development of lead removal methods [19] its industrial usage is, in fact, growing [20], therefore the lead influence on the living organisms is still an important issue. In this research, the vacuolar membrane of *Beta vulgaris* was selected, because the structure and function of this membrane is well-known [21–24] and it can be used as a model membrane. The basic ion currents in vacuolar membranes of higher plants are conducted by the nonselective slow activated cationic channels (SV), fast activated channels (FV), high-selective vacuolar potassium channels. FV channels, in contrast to SV channels, are active at physiological concentration of cytoplasmic Ca^{2+} and blocked by calcium ions, while increasing their concentration in cytoplasm (above 1 μM) [24–26]. It was found that FV channels are also sensitive to the redox potential [27] and other physiological factors [28]. The sensitivity of SV channels to Ca^{2+} ion concentration is related to their involvement in Ca^{2+} homeostasis of the cells [29]. In the conditions most commonly used in researches carried out in patch-clamp technique (symmetrical K^+ ion concentration and millimolar lumen concentration of Ca^{2+}) SV channels are activated at positive membrane potentials. It is worth noticing that in vitro (in patch-clamp experiments) SV channels are activated by the positive (nonphysiological) membrane voltages, whereas in vivo these channels are, in theory, completely deactivated. In the experiments the trimethyllead chloride (Met_3PbCl) was used since its influence was investigated by standard patch-clamp analysis methods [30]. Moreover, it is soluble in water, so it can be accumulated in the root tissue through the soil environment. In this paper, a new aspect of lead toxicity is verified therefore relatively high lead compound concentration was used.

In the experimental part of the study, the patch-clamp technique was used [31] and the long term correlations of the open—close state time series investigated by the rescaled range analysis (R/S) and detrended fluctuation analysis (DFA). The R/S analysis was proposed by Hurst [32] to analyse changes of river levels but the method appeared to be very useful in the various researches on time series among which were ion channel time series recordings [33, 34]. The main outcome of the R/S analysis is the Hurst exponent, which describes correlation properties of the signal. DFA introduced by [35] is an alternative method to measure Hurst exponent, which was successfully applied to ionic channel analysis [36–39]. In the case of infinite time series, both techniques are expected to give the same results, however, in finite cases the question which one gives a better estimation of the Hurst exponent is still a controversy [40, 41].

Materials and methods

The experiment

Electrophysiological measurements presented in the paper were carried out on patches of red beet (*Beta vulgaris* L.) tonoplast. The plants used for the study came from organic farming. Vacuoles were isolated from taproots according to the method described by Coyaud et al [21]. Fresh root was cut with a sharp tool and then washed with the incubation solution, enabling the vacuoles to be directly extruded into the recording chamber (1 ml in volume).

The control bath solution was: 100 mM KCl, 2 mM $MgCl_2$, 0.1 mM $CaCl_2$, 5 mM MES, 5 mM TRIS and 400 mM sorbitol; pH 7.5 (adjusted by 0.1 N NaOH), osmolarity 656 mOsm. Pipettes were filled with a solution of composition: 100 mM KCl, 2 mM $MgCl_2$, 1 mM $CaCl_2$, 5 mM MES, 5 mM TRIS, 340 mM sorbitol, pH 5.5, 587 mOsm. The osmolarity of all the

solutions used was adjusted under the control of cryoscopic osmometer Semi-Micro_Osm-ometer K-7400, (Knauer, Germany).

Electrophysiological measurements were carried out using EPC-7 plus amplifier equipped with data acquisition hardware, Instru TECH LIH 8+8 (List-Medical-Electronic, Darmstadt, Germany) and software Patch-Master (HEKA Electronic, Lambrecht, Germany). Signal was probed every 50 μs and analog filtered by Bessel filter (in the device) at cut-off frequency 1 kHz. Transmembrane voltage was controlled in voltage clamp condition. Membrane polarity was consistent with Bertl et al. convention [42].

Micropipettes were made from borosilicate glass tubes (Kimax-51, Kimble Products, Toledo, Ohio, USA) using two stage puller (Model L/M-3-PA, List medical, Germany), fire polished with a microforge CPZ 101 (List medical, Germany) and coated with Sylgard (Dow Corning, Midland, MI, USA). The resistance of micropipette filled with a pipette solution was in the range of about 2–4 MΩ, and seal resistance 4–20 GΩ.

Microscopic currents were recorded in the inside-out configuration (cytosolic side out patch), which was obtained in the following way. First starting from the vacuole-attached con-figuration and using electroporation of membrane within a micropipette (applying short-time voltage pulse in the range of 300 to 900 mV), a whole vacuole system was obtained. Next, after detachment of the patch from tonoplast with a quick micropipette movement, we got the inside-out configuration.

Measurements protocol was as follows. The voltage was maintained as a constant function in a given time interval. Starting from zero (10 s) the potential was subsequently changed to -50 mV (operating voltage) and kept on this value for 10 seconds, after which it was switched back to zero for another 10 s. Such cycle was repeated with the gradation of operating voltage every 10 or 20 mV in the range (- 50 mV, 100 mV) and in some experiments only 80 and 100 mV. Effect of 100 μM trimethyllead (Met$_3$PbCl) on SV channels activity were studied. Due to the duration of our experiments (from a few to several mins) we decided to use higher lead concentration than those present in nature). During experiments, the control solution was changed for a new one of the same composition, supplemented by trimethyllead.

After doing several such series of records in the control the same vacuole was incubated in a solution containing trimethyllead. The exchange of incubated media was carried out by con-tinuous perfusion of the measuring chamber using an infusion pump (SP 200, World Preci-sion Instruments, USA). Replacement time of the incubation solution was approx. one minute.

Experiments were carried out in the room temperature (22±1˚C). For the data analysis, the ion current recordings were pre-normalized by subtracting the leak currents (the zero offset).

Data analysis

Data from 28 different vacuolar patches were analyzed. On most of them due to the instability of the patch-micropipette layout for a longer period (over ca. 10 minutes), the data comes from individual protocols (control and then solution supplemented with Met$_3$PbCl). If the patch was sufficiently stable, the measurement protocol was repeated several times in control and then in the presence of a modifier. The analysis included a total of 80 individual traces (each of them with a duration of 10 seconds), 40 for the control and 40 for the modifier, respectively. The activity of SV channels in the membrane was usually determined by record-ing the macroscopic current (in the whole vacuole system, before forming the inside out). This current shows characteristic typical for SV channels: sigmoidal time course with activation constant of seconds and rectifying current-voltage characteristics (data not shown). Recorded microscopic currents were consistent with what is observed in the whole system and in good

agreement with the data of other authors—conductivity of single-channel—72 pS and voltage-dependent gating (activity were observed at a voltage above 40 mV).

In the experiment, the current through an ion channel was measured for the following external potential: (-50 mV, 100 mV), with step 10 mV. However, the best results with clearly open and closed states were observed for the external potential equal 80 mV and these time series were analysed within this paper. The experiment was repeated 40 times (standard bath solution) and 40 times in the bath solution with 0.1 mM of Met_3PbCl.

Each analysed time series consists of $2 \cdot 10^5$ data points with the resolution of 0.05 ms (10 s recordings). The time series registered during the patch-clamp measurements were verified against the presence of more than one active channel and stationarity of the ionic channel recordings.

The problem of sometimes observed instability of the functioning of the channel, in particular, spontaneous loss of channel activity over time called run-down is not sufficiently recognized in the literature so far. It should be emphasized that this phenomenon is rather not the result of the destruction of the channel structure because the current through a single channel does not change, while its activity is temporarily lost. Furthermore, the latter is also correlated with the loss of macroscopic current.

A large number of ion channels, in particular potassium channels, are regulated by substances contained in the cytosol, such as nucleotides, calcium ions and other signaling molecules. In patch clamp experiments, homeostasis of membrane contact with the intracellular environment is disturbed by washing out these substances as a result of membrane perforation (whole-cell) or patch detachment.

In general, the molecular mechanism responsible for the run down has not been well understood, however, this phenomenon has been thoroughly studied on L-type calcium channels. A binding site (C-terminal sequence 1572–1651 of the α_{1C} subunit for the intracellular modulator, calpastatin, responsible for the run down effect was found in this channels [43].

In the case of SV channels of higher plants [44, 45] observed run-down of ion current was rather low on the level of 18%–19% within several minutes of observation. Much higher influences were observed in animal cells [46].

Some solution to the run down problem in patch clamp experiments (in whole cell configuration) seems to be the use of pore-forming substances, such as antibiotics (amphotericin B, nystatin). The pores thus created allow electrical contact between the micropipette solution and the interior of the cell without disturbing its homeostasis, due to the possibility of only small ions penetrating the pore formed [47]. Another method of the run-down prevention is the usage of dedicated compounds e.g. by adding DTT [48], ATP [49] or DTP [50], however none of the authors does not discuss the recovery of statistical properties of the ion channels. Therefore, the protocol, which allowed to analyse ion current without additional components was chosen.

The probability distribution functions (see Sec. *Probability density of ionic current*) of the registered signals were obtained and the cases with two maxima chosen i.e. with one active ionic channel. The stationarity of the time series was verified by the bootstrap method [51] and the time series with fluctuations of the 90 and 10 percentile exceeding 5% were rejected. After the inspection of the data, the analysis was continued on the 35 recordings at the standard bath solution and 23 time series at the solution with 0.1 mM of Met_3PbCl. The examples of the registered time series are presented in Fig 1. For the chosen time series the value of the threshold was obtained and the current time series were transformed into the dwell-time series. Finally, the long-range correlations were investigated by R/S and DFA analyses.
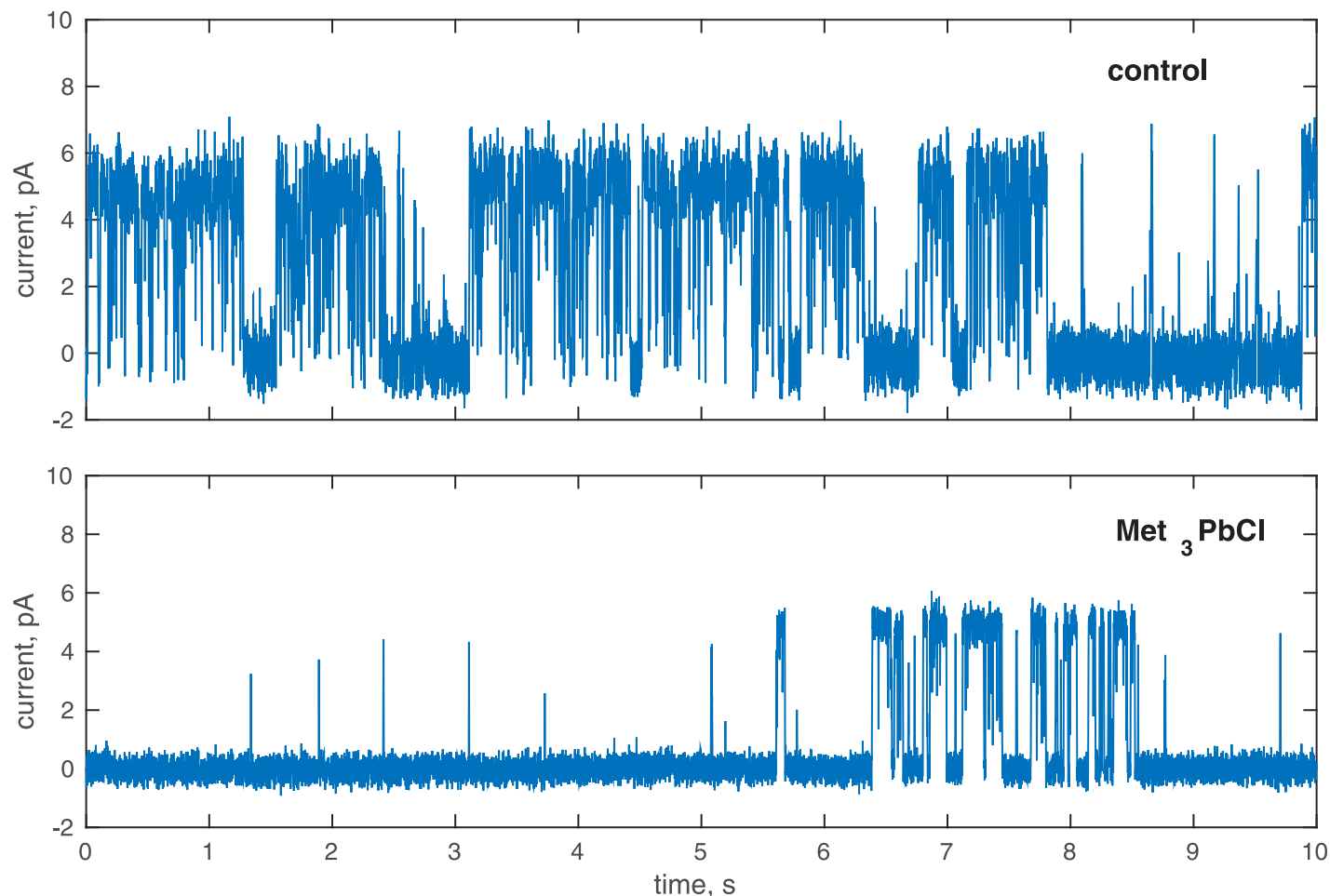
Fig 1. An example of the registered ionic current in the control solution and in the presence of Met₃PbCl. Membrane potential was 80 mV.

Probability density of ionic current

A histogram is the simplest probability functions approximation, however, the results are rather rough. In order to resolve this ambiguity the kernel density estimator with the Gaussian kernel density was used [52, 53]. The examples of the obtained probability distribution functions (PDF) are presented in Fig 2. The procedure of the threshold current approximation proposed by [36, 37] was modified due to the number of time series analysed (more than a thousand samples). The threshold current between the open and close states was found as a local minimum of the fitted PDF. Finally, the ionic current signal was converted into the dichotomous signal (open and close states) and the time series of open and close states times were obtained. The example of the converted time series is presented in Fig 3.

R/S analysis

The detailed description of rescaled range analysis (R/S) can be found in various books on the fractal analysis e.g. [54]. Here the key elements are presented. Let denote the time series by A and its elements as $\{a_1, a_2, \ldots, a_n\}$, then
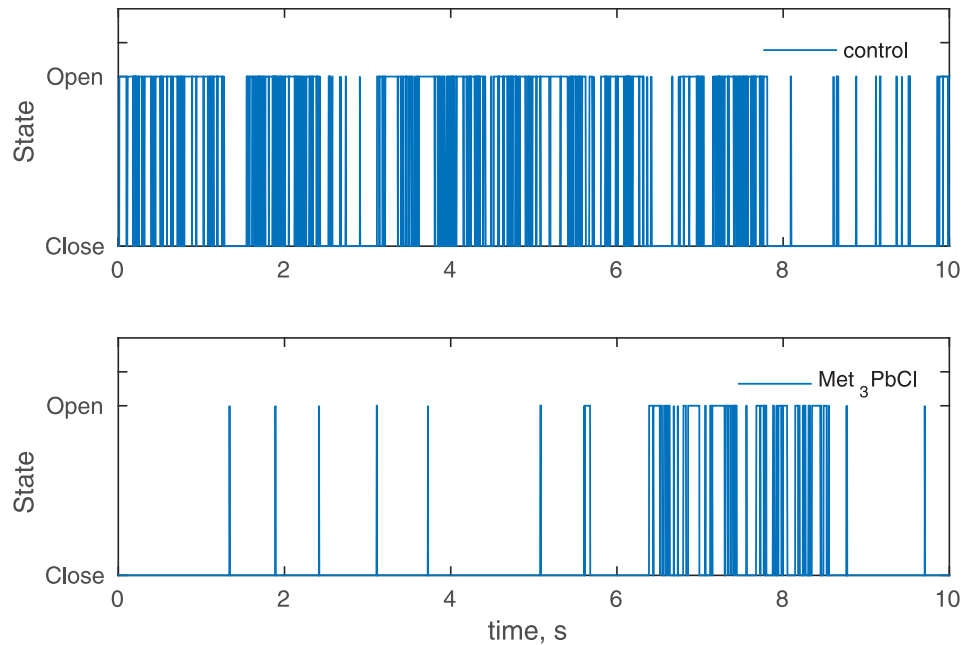
Fig 2. PDF's of the time series presented in Fig 1 fitted by the kernel distribution function. Membrane potential was 80 mV.

1. Create the mean adjusted time series $b_i = a_i - \langle A \rangle$, where $\langle A \rangle$ is the mean value of the time series.

2. Calculate cumulative time series: $c_t = \sum_{i=1}^{t} b_i$, $t = 1, 2, 3 \ldots, n$.

3. Create the range series: $r_t = \max\{c_1, c_2, \ldots, c_t\} - \min\{c_1, c_2, \ldots, c_t\}$, $t = 1, 2, 3 \ldots, n$.

4. Create the standard deviation time series: $s_t = \sqrt{\frac{1}{t}\sum_{i=1}^{t}(a_i - u)}$, where $t = 1, 2, 3 \ldots$, and $u = \frac{1}{t}\sum_{i=1}^{t} a_i$.

5. Calculate R/S time series: $\left(\frac{R}{S}\right)_t = \frac{r_t}{s_t}$.

6. Finally the power law $\left(\frac{R}{S}\right)_t \sim t^H$ is fitted to the transformed time series and the Hurst exponent (H) estimated.

   In the case of the persistent time series $H > \frac{1}{2}$, while for the antipersistent time series $H < \frac{1}{2}$.

DFA analysis

The detrended fluctuation analysis (DFA) is an alternative method for Hurst exponent estimation. Details can be found in e.g. [55, 56].

1. The procedure starts form the transformation of a time series A (of N samples), $\{a_1, a_2, \ldots, a_N\}$ into a cumulated mean adjusted time series: $X_t = \sum_{i=1}^{t}(a_i - \langle a_i \rangle)$, then

2. the time series is divided into n equal size boxes, and

3. in every box a local trend y_n is fitted. In fact any function could be used to approximate the trend, but in practice the linear function is the most popular choice. The higher order polynomials are rarely used e.g. [57].
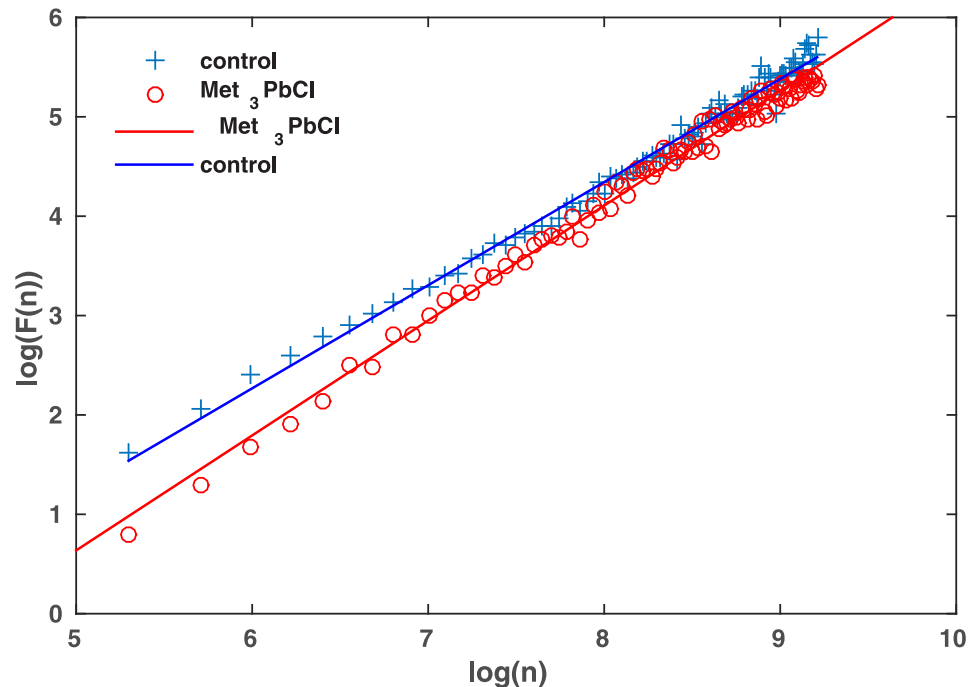
Fig 3. The dichotomous open-close state signal obtained from the signal presented in Fig 1. Membrane potential was 80 mV.

4. The trend is subtracted from the integrated signal and its fluctuation calculated:
$F(n) = \sqrt{\frac{1}{N}\sum_{k=1}^{N}[X_k - y_n(k)]^2}$. $F(n)$ is calculated for all possible sizes of boxes.

5. Finally the power law function $F(n) \sim n^\alpha$ is fitted. (Usually by fitting linear function to the log-log transformed plot.)

The interpretation of the results is: (i) if $\alpha < 0.5$, then the anti-correlated time series is observed, (ii) $\alpha \simeq 0.5$ the uncorrelated white noise is measured, (iii) $\alpha > 0.5$ the correlated time series is observed.

The main difference between R/S and DFA is that R/S removes a constant trend from the data while DFA subtracts the linear trend.

Results

One example of DFA analysis is presented in Fig 4. The results of the DFA and R/S analysis are presented in Tables 1 and 2. The Hurst exponents for both methods applied and in all considered experimental data significantly exceed the value 0.5 showing the existence of long-range correlations of open-close states. Analysing the results obtained by R/S and DFA it is observed that the Hurst exponents calculated by R/S analysis are smaller than those received by DFA. The difference between mean values of the Hurst exponent at R/S analysis is equal 0.07 while for DFA analysis 0.13. However, the most important result is that the observed changes in long-correlation being the result of the Met_3PbCl presence are statistically significant. The one way ANOVA analysis have been applied and the p-value of the null hypothesis stating that there is no difference of the Hurst exponent of the ion current in the control solution and in the presence of Met_3PbCl is equal $1.2 \cdot 10^{-5}$ at R/S analysis and even $6.4 \cdot 10^{-13}$ at DFA analysis. Therefore, the null hypothesis is rejected and the alternative accepted. Due to the uni-vocal
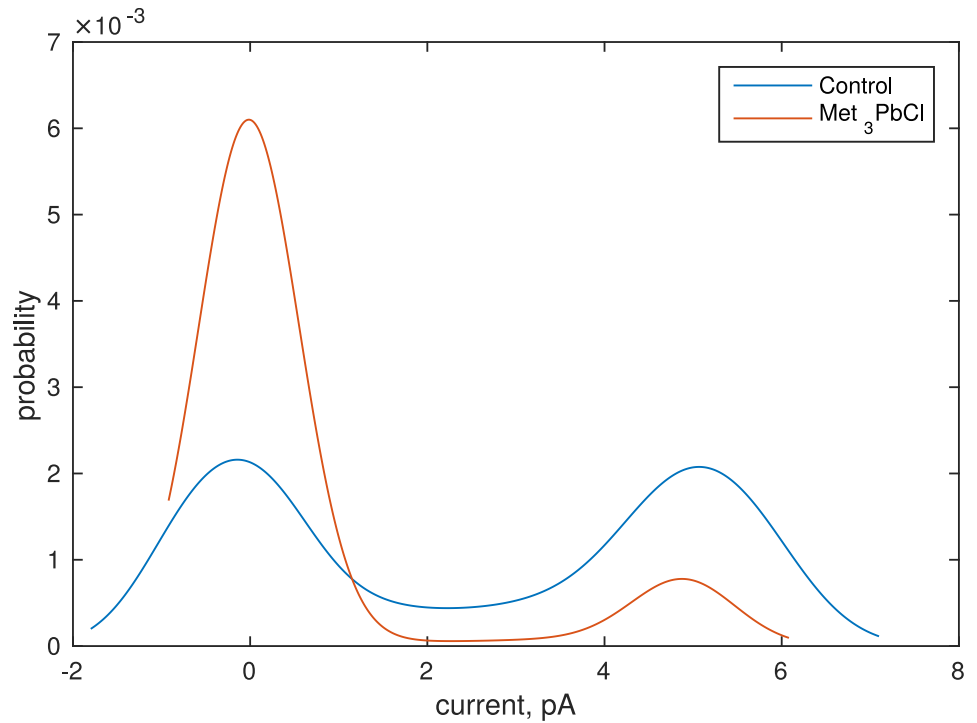
Fig 4. The DFA of the signal presented in Fig 1. n denotes the box size, while $F(n)$ the fluctuations. Membrane potential was 80 mV.

https://doi.org/10.1371/journal.pone.0229433.g004

Table 1. The mean value and the standard deviation of the Hurst exponent approximation obtained by R/S analysis. Additionally the statistical significance of the difference between means is presented. Membrane potential was 80mV.

	control	Met₃PbCl
mean	0.85	0.78
std	0.03	0.03
ANOVA p-value		$1.2 \cdot 10^{-5}$

https://doi.org/10.1371/journal.pone.0229433.t001

result, there comes the question on the possible mechanism of the Met_3PbCl influence. This problem is analysed in the following section.

Channel model

Within the present work, the long memory effects are investigated therefore the problem of developing a model is interesting itself and the reader may refer to [58]. Within the present

Table 2. The mean value and the standard deviation of the Hurst exponent approximation obtained by DFA analysis. Additionally the statistical significance of the difference between means is presented. Membrane potential was 80 mV.

	control	Met₃PbCl
mean	1.05	0.93
std	0.07	0.13
ANOVA p-value		$6.4 \cdot 10^{-13}$

https://doi.org/10.1371/journal.pone.0229433.t002

analysis, the model developed in [58] is used. For the convenience of the reader, the key model features and the algorithm generating the dwell time series are presented here. The main advantage of the model is that it does not only reconstruct the desired open-close state probability but also generates appropriate autocorrelations among the states. The model is defined on a 1-dim lattice with given boundaries and the arbitrarily chosen point dividing the lattice space into open and close states. The open-close states time series are generated by random walk on a lattice with an external potential and a threshold between open and close states spaces.

The conformational space is defined on 1-dim lattice with N-nodes. The ends of the lattice are denoted as B_{MIN} and B_{MAX}. The reaction coordinate (RC) corresponding to the state of the channel gate is placed on the lattice and at each step of the simulation RC can be moved by one node. The range of the accessible nodes is limited by movable boundaries $B1$ and $B2$. The motion of these boundaries corresponds to the thermal fluctuations in the membrane thickness and internal strains within protein segments influencing the conformational space of open and close states. They are synchronised in directions (i.e. if the spaces corresponding to the open states shrinks the same happens to the close states space). At the centre of the lattice the threshold point (TP) is placed. This point divides the conformational space into open and close spaces. During the simulations, there are two movable elements: RC, B1 and B2 (B1 and B2 are synchronised). Since there is a significant difference in mass of the fluctuating membrane and the mass of the putative activation gate the fluctuation rate of both parameters are on different time scales. The change of the boundaries is performed after a given number of iterations according to the formula:

$$D_B = \frac{D_{RC}}{600},\tag{1}$$

which was estimated on the experimental data (D_B is the boundary diffusion coefficient while D_{RC} denotes reaction coordinate diffusion coefficient) [58]. The RC perform on the lattice a biased random walk. The probabilities of decreasing (q) or increasing (p) position of RC are given by the Eqs (2) and (3) [59].

$$q = \frac{1}{2} + \frac{\Delta U}{4kT}\tag{2}$$

$$p = \frac{1}{2} - \frac{\Delta U}{4kT}\tag{3}$$

Where k is the Boltzmann constant, T the absolute temperature and ΔU a potential energy difference within a lattice step centred around RC. In order to recover appropriate drift force (being the result of the external potential on the membrane e.g. $V = 80mV$) the potential $U(x)$ is postulated in the following form [58]:

$$\begin{cases} U(x) = (x - B1) \cdot A + U_{B1}; x \in \langle B1; TP - 1.5) \\ U(x) = (x - (TP - 1.5)) \cdot B + U_{TP-1.5}; x \in \langle TP - 1.5; TP) \\ U(x) = (x - TP) \cdot (-B) + U_{TP}; x \in \langle TP; TP + 1.5 \rangle \\ U(x) = (x - (TP + 1.5)) \cdot A + U_{TP-1.5}; x \in \langle TP + 1.5; B2) \\ A = \frac{U_{TP-1.5} - U_{B1}}{TP-1.5 - B1} \\ B = \frac{U_{TP} - U_{TP-1.5}}{TP - (TP-1.5)} \end{cases},\tag{4}$$

where $B1$ and $B2$ are the locations of the left and right boundaries, respectively, TP is the

threshold point position, U_{B1}, U_{TP} and $U_{TP-1.5}$ are values of the potential at the given points. It is also assumed that the potential changes its value linearly and A and B are the slope coefficients defining potential slopes on the intervals $(B1; TP - 1.5)$ and $(TP - 1.5; TP)$, respectively. After each iteration step the position of RC is checked and if it is on the left of TP then open state is recorded in generated time series otherwise the close state is registered.

The lattice size was set to $2B_{MAX} + 1 = 29$ nodes—determining the maximum size of the open and closed state spaces. The starting position was set at the closed neighbourhood of the threshold TR ($RC = \{-1, 0, 1\}$). In fact, the choice of the initial position does not influence the results of simulations. Assuming that the iteration step of the simulation necessary to move RC is equal to 1 then the boundaries positions $B1$ and $B2$ were changed every 600 iteration steps to satisfy Eq (1).

While performing the simulations the experimental limitations were taken into account: the ion channel time series were of limited size (i.e. $2 \cdot 10^5$ data points), the statistical parameters of ion channel time series (i.e. open probability, and Hurst exponent obtained by R/S and DFA analyses) have a dispersion—due to the biological variability and time series size. Moreover, the theoretical model is in fact a non-linear model with four parameters. Therefore, the possibility that there are more than one solution (a parameter set under which the simulations generate time series of required properties) should not be excluded. In order to find multiple solutions, instead of optimization technique [58] the scanning of the state space was performed. The initial parameter combination were $\{U_{B1} = 1kT, U_{B2} = 1kT, U_{TP} = 1kT, U_{TP-1.5} = 1kT\}$ till $\{U_{B1} = 25.5kT, U_{B2} = 25.5kT, U_{TP} = 25.5kT, U_{TP-1.5} = 25.5kT\}$ with resolution $0.5kT$, so $6.25 \cdot 10^6$ states where examined. The temperature was set $T = 300K$. The others parameters agreed with [58] ($B_{MAX} = -B_{MIN} = 14$, $TP = 0$).

Since the Hurst exponent analysis (both R/S and DFA) are computationally complex the simulations were divided into two steps. During the first scan the opening probabilities were calculated and after filtering the results such that the opening probabilities were in the interval *average opening probability ± standard deviation*, then the simulations were repeated for the filtered parameter set. At this stage for each set of parameters twelve samples of time series were generated and the DFA and R/S analyses were performed. Finally the parameters sets matching the results obtained on the experimental data (Tables 1 and 2) were collected. The simulation parameters that generates time series with expected open probability and Hurst exponent are presented in Tables 3 and 4.

The simulations parameters of the numerical model generating dwell time series (Table 3) of the properties similar to the ionic current time series at the presence of Met$_3$PbCl are characterised by low values of the considered set of UB1 potential and are at the range from 1 kT up to 8.5kT. The potential threshold at TP takes high values at the interval from 19.5kT up to 25.5kT. Similar values are observed for UTP15, which is responsible for the potential just before and after TP, and the values are in the range 20.5kT to 25.5kT. The difference between UTP and UTP15 is relatively small considering the range of the simulation parameters and vary from -1kT up to 2kT, but most of the collected simulation parameters are characterised by the positive difference between UTP and UTP15. The significant spread between UB1 and UTP15, which in fact "keeps" RC at the close state side of the lattice. It is also noticeable that within the chosen range of simulation parameters there are more parameters sets which reconstruct the behaviour of the ionic channel at the presence of Met$_3$PbCl than in control solution. Another interesting observation is the difference between the Hurst exponent obtained by R/S and DFA methods. In Table 3 the Hurst exponent obtained by R/S is smaller than received by DFA. The similar difference is observed for experimentally observed time series. Although, both methods should give similar results it is true only in an infinite time series [40]. In the case of real observations, there is a "sample size effect" and both methods give different results.

Table 3. The parameters (in kT units) of the theoretical model reconstructing time series of the properties of the ion channel in the presence of Met₃PbCl.

parameters (UB1; UB2; UTP; UTP15)	open prob. $p\pm\sigma$	H by R/S $h\pm\sigma$	H by DFA $h\pm\sigma$
(1; 1; 24.5; 24)	0.019±0.005	0.78±0.02	1.19±0.03
(1; 1.5; 25.5; 25.5)	0.018±0.004	0.77±0.02	1.22±0.03
(1; 10.5; 24.5; 24)	0.020±0.006	0.78±0.02	1.19±0.03
(1; 12.5; 24; 22.5)	0.024±0.006	0.78±0.02	1.13±0.03
(1; 14; 24.5; 25.5)	0.017±0.004	0.77±0.03	1.24±0.13
(1; 16; 23; 23)	0.019±0.004	0.77±0.03	1.22±0.03
(1; 17.5; 24.5; 24.5)	0.018±0.005	0.77±0.02	1.21±0.03
(1; 22; 25.5; 25)	0.021±0.007	0.77±0.02	1.19±0.04
(1; 24; 25; 24.5)	0.021±0.004	0.77±0.02	1.19±0.03
(1; 24; 25.5; 24)	0.021±0.007	0.78±0.02	1.14±0.03
(1.5; 5; 23.5; 23)	0.019±0.006	0.77±0.02	1.19±0.03
(1.5; 5; 25.5; 25.5)	0.018±0.005	0.78±0.02	1.20±0.03
(1.5; 11; 22.5; 22.5)	0.018±0.005	0.77±0.02	1.22±0.03
(1.5; 8.5; 25; 24)	0.021±0.006	0.78±0.02	1.17±0.05
(1.5; 9.5; 21.5; 23)	0.016±0.005	0.77±0.02	1.25±0.05
(1.5; 13.5; 25; 23.5)	0.023±0.005	0.78±0.02	1.15±0.04
(1.5; 14.5; 21.5; 22)	0.017±0.004	0.77±0.02	1.23±0.03
(1.5; 20.5; 22; 23)	0.017±0.005	0.77±0.02	1.24±0.03
(1.5 15 23.5 24)	0.018±0.006	0.77±0.02	1.23±0.03
(1.5; 15; 25; 24.5)	0.020±0.004	0.77±0.02	1.20±0.03
(2; 7.5; 24; 23.5)	0.018±0.006	0.77±0.02	1.19±0.03
(2; 9; 24; 23)	0.022±0.007	0.78±0.02	1.17±0.03
(2; 13; 24.5; 22.5)	0.023±0.006	0.78±0.02	1.11±0.04
(2; 15; 20.5; 19)	0.019±0.006	0.77±0.02	1.14±0.04
(2; 16; 23.5; 23.5)	0.021±0.007	0.77±0.02	1.22±0.03
(2; 23; 21.5; 20.5)	0.020±0.007	0.77±0.02	1.17±0.03
(2; 24; 21.5; 21)	0.021±0.005	0.77±0.02	1.19±0.02
(2.5; 19.5; 24; 22.5)	0.025±0.007	0.78±0.02	1.14±0.03
(2.5; 21; 24.5; 25.5)	0.017±0.004	0.77±0.02	1.25±0.03
(2.5; 24; 24; 24)	0.018±0.006	0.78±0.02	1.2±0.03
(3; 5; 24; 23)	0.020±0.006	0.77±0.02	1.16±0.04
(3; 6.5; 24; 24.5)	0.016±0.005	0.77±0.02	1.23±0.03
(3; 11; 22; 22.5)	0.018±0.005	0.77±0.02	1.22±0.03
(3; 12.5; 24; 23)	0.021±0.006	0.78±0.02	1.16±0.04
(3; 14; 22.5; 22)	0.018±0.006	0.77±0.02	1.19±0.04
(3; 15.5; 24.5; 23.5)	0.020±0.007	0.77±0.02	1.17±0.03
(3; 17; 24; 23.5)	0.019±0.006	0.77±0.02	1.20±0.03
(3; 17.5; 25.5; 25.5)	0.020±0.006	0.77±0.02	1.21±0.03
(3.5; 17.5; 24.5; 24.5)	0.018±0.005	0.77±0.02	1.22±0.03
(4.5; 25; 24; 22.5)	0.021±0.007	0.78±0.02	1.14±0.03
(5; 5.5; 25.5; 25)	0.017±0.004	0.77±0.02	1.19±0.03
(5; 25; 20.5; 20.5)	0.017±0.004	0.78±0.02	1.21±0.03
(6.5; 1.5; 25.5; 25)	0.020±0.005	0.77±0.02	1.19±0.02
(8.5; 13; 24.5; 24.5)	0.020±0.006	0.78±0.02	1.21±0.03

Table 4. The parameters (in kT units) of the theoretical model reconstructing time series of the properties of the ion channel in the control solution.

parameters (UB1; UB2; UTP; UTP15)	open prob. $p\pm\sigma$	H by R/S $h\pm\sigma$	H by DFA $h\pm\sigma$
(4.5; 23.5; 1; 3)	0.447±0.038	0.80±0.03	0.77±0.03
(10.5 24 7.5 9.5)	0.413±0.023	0.79±0.02	0.77±0.03
(21.5; 11.5; 16; 18.5)	0.485±0.033	0.82±0.03	0.85±0.04
(23.5; 5; 19; 21.5)	0.409±0.029	0.80±0.02	0.80±0.02
(25.5; 23; 20; 22.5)	0.489±0.046	0.81±0.03	0.84±0.03

https://doi.org/10.1371/journal.pone.0229433.t004

However, the difference between Hurst exponent obtained by both methods is analogous in experimental and simulated time series.

The parameters of the model reconstructing the time series of the ion channel in the control solution are presented in Table 4. In this case, the UB1 potential takes much higher values, which lies in the interval 4.5kT to 25.5kT however the high values (>20kT) prevail. Particularly interesting is the analysis of the threshold potentials UTP and UTP15. These potentials do not define a threshold but rather a potential well, which forms a "trap" for RC with the depth in the range 2kT and 2.5kT. In three out of five sets have potential UB2>UB1.

Discussion

The transport mechanisms, within ion current are crucial to cell biology. The recent researches indicate long-range correlations in the open-close state time series of the single ion channel currents [36–39]. The main aim of the present study is to verify whether the reported long-range correlations are sensitive to the presence of organolead. In the analysis, the ionic time series were registered by the patch-clamp technique and subsequently transformed into the dichotomous signal, which was finally converted into the dwell time series. The transformed series were investigated by R/S and DFA analyses. Besides the result that the open-close state time series of SV channels of the vacuolar membrane is persistent ($H > 0.5$), which was also reported in similar studies [39, 60] it has been shown that the long-range correlations are sensitive to the presence of Met$_3$PbCl. This result is new and provides two important observations: firstly the long correlations in ion channels currents might be sensitive to various compounds and more specific is that the lead influences such correlations. The origins of the long-range correlations are still a subject of investigations. The observed phenomenon was further investigated by the numerical model reconstructing dwell time series of required properties. The sets of model parameters generating the time series of the characteristic of the ion channel current at the control solution and at the presence of Met$_3$PbCl were found. The most important difference of the sets was that those reconstructing the organolead compound influence were characterised by significantly lower values of UB1 potential such that instead of potential well the threshold is observed.

It should be stressed that the disturbance of the long-term correlations could be considered as a destabilization element, which in consequence may results in an increase of vulnerability of the organisms.

Besides the direct result of our study i.e. the observation that Met$_3$PbCl change long range correlation in ion channel current we would like to draw attention on another problem. In physical systems the existing correlations are the results of interactions. So, if the long memory of ion channels has biological significance than there exists a mechanism responsible for it. This hypothesis is very intriguing because on the microscopy level there are not many reasons that the molecules might "remember" its previous state. On the other hand, this study shows

that some compounds indeed change long memory parameters, so the ion channel models should include mechanisms properly reconstructing also this aspect.

The obtained results open a new area of research showing that long correlations of ion channels may be influenced by various compounds and this aspect should be also a subject of investigations.

Author Contributions

Conceptualization: Janusz Miśkiewicz, Wanda Balińska-Miśkiewicz.

Data curation: Zenon Trela.

Funding acquisition: Janusz Miśkiewicz.

Investigation: Zenon Trela, Zbigniew Burdach, Waldemar Karcz.

Methodology: Zenon Trela.

Software: Janusz Miśkiewicz.

Visualization: Janusz Miśkiewicz.

Writing – original draft: Janusz Miśkiewicz.

Writing – review & editing: Janusz Miśkiewicz, Wanda Balińska-Miśkiewicz.

References

1. Miśkiewicz J, Trela Z, Przestalski S, Karcz W. Superstatistics analysis of the ion current distribution function: Met3PbCl influence study. European Biophysics Journal. 2010; 39(10):1397–1406. https://doi.org/10.1007/s00249-010-0594-y PMID: 20354691

2. Craig PJ. Organometallic Coumpounds in the Environment. Willey, Chister; 2003.

3. Carruyo I, Fernandez Y, Marcano L, Montiel X, Torrealba Z. Correlation of Toxicity with Lead Content in Root Tip Cells (Allium cepa L.). Biol Trace Elem Res. 2008; 125:276–285. https://doi.org/10.1007/s12011-008-8175-y PMID: 18636231

4. Day M, Cooney JD, Shen Z. Pyrolysis of automobile shredder residue: an analysis of the products of a commercial screw kiln process. Journal of Analytical and Applied Pyrolysis. 1996; 37:49–67. https://doi.org/10.1016/0165-2370(96)00938-2

5. Andreottola G, Dallago L, Ferrarese E. Feasibility study for the remediation of groundwater contaminated by organolead compounds. Journal of Hazardous Materials. 2008; 156:488–498. https://doi.org/10.1016/j.jhazmat.2007.12.044 PMID: 18242831

6. Bragadin M, Marton D, Manente S. Trilkyllead compounds induce the opening of the MTP pore in rat liver mitochondria. Journal of Inorganic Biochemistry. 2007; 101:876–878. https://doi.org/10.1016/j.jinorgbio.2007.01.016 PMID: 17368777

7. White LD, Cory-Slechta DA, Gilbert ME, Tiffany-Castiglioni E, Zawia NH, Virgolini M, et al. New and evolving concepts in the neurotoxicology of lead. Toxicology and Applied Pharmacology. 2007; 225:1–27. https://doi.org/10.1016/j.taap.2007.08.001 PMID: 17904601

8. Silbergeld EK. Facilitative mechanisms of lead as a carcinogen. Mutation Research. 2003; 533:121–133. https://doi.org/10.1016/j.mrfmmm.2003.07.010 PMID: 14643416

9. Cairney S, Maruff P, Burns C, Currie B. The neurobehavioral consequences of petrol (gasoline) sniffing. Neuroscience and Biobehavioral Reviews. 2002; 26:81–89. https://doi.org/10.1016/s0149-7634(01)00040-9 PMID: 11835986

10. Lespes G, Marcic C, Heroult J, Le I, Denaix L. Tributyltin and triphenyltin uptake by lettuce. Journal of Environmental Management. 2009; 90:S60–S68. https://doi.org/10.1016/j.jenvman.2008.07.019 PMID: 18951698

11. Michalzik B, Ilgen G, Hertel F, Hantsch S, Bilitewski B. Emission of organo-metal compounds via the leachate and gas pathway from two differently pre-treated municipal waste materials—A landfill reactor study. Waste Management. 2007; 27:497–509. https://doi.org/10.1016/j.wasman.2006.02.018 PMID: 16714103

12. Agency for Toxic Substances and Disease Registry; 2018. http://www.atsdr.cdc.gov/.

13. Mitra P, Sharma S, Purohit P, Sharma P. Clinical and molecular aspects of lead toxicity: An update. Critical reviews in clinical laboratory sciences. 2017; 54(7-8):506–528. https://doi.org/10.1080/10408363.2017.1408562 PMID: 29214886

14. Schofield K. The metal neurotoxins: an important role in current human neural epidemics? International journal of environmental research and public health. 2017; 14(12):1511. https://doi.org/10.3390/ijerph14121511

15. Fatmi Z, Sahito A, Ikegami A, Mizuno A, Cui X, Mise N, et al. Lead Exposure Assessment among Pregnant Women, Newborns, and Children: Case Study from Karachi, Pakistan. International Journal of Environmental Research and Public Health. 2017; 14(4). https://doi.org/10.3390/ijerph14040413 PMID: 28406467

16. Staniak S. Źródła i poziom zawartości ołowiu w żywności. Polish Journal of Agronomy. 2014; 19:36–45.

17. Küpper H. Lead Toxicity in Plants. In: Lead—Its Effects on Environment and Health. vol. 17. Berlin, Boston: De Gruyter; 2017. p. 491–500.

18. Needleman HL. The Removal of Lead from Gasoline: Historical and Personal Reflections. Environmental Research Section A. 2000; 84:20–35. https://doi.org/10.1006/enrs.2000.4069 PMID: 10991779

19. Tylkowski B, Jastrzeb R. Smart Capsules for Lead Removal from Industrial Wastewater. In: Lead—Its Effects on Environment and Health. vol. 17. Berlin, Boston: De Gruyter; 2017. p. 61–78.

20. Lead I, Group ZS. Lead and Zinc Statistics; 2019. http://www.ilzsg.org/static/statistics.aspx.

21. Coyaud L, Kurkdijan A, Kado R, Hedrich R. Ions channels and ATP-driven pumps involved in ion transport across the tonoplast of sugarbeet vacuoles. Biochim Biophys Acta. 1987; 902:263–268. https://doi.org/10.1016/0005-2736(87)90304-X

22. Hedrich R, Flugge U, Fernandez MJ. Patch-clamp studies of ion transport in isolated plant vacuoles. FEBS Lett. 1986; 204:228–232. https://doi.org/10.1016/0014-5793(86)80817-1

23. Miedema H, de Boer AH, Pantoja O. The gating kinetics of the slow vacuolar channel. A novel mechanism for SV channel functioning? J Membrane Biol. 2003; 194:11–20. https://doi.org/10.1007/s00232-003-2022-z

24. Hedrich R, Neher RE. Cytoplasmic calcium regulates voltage-dependent ion channels in plant vacuoles. Nature. 1987; 329:833–836. https://doi.org/10.1038/329833a0

25. Tikhonova L, Pottosin I, Dietz KJ, Schönknecht G. Fast-activating cation channel in barley mesophyll vacuoles. Inhibition by calcium. Plant J. 1997; 11:1059–1070. https://doi.org/10.1046/j.1365-313X.1997.11051059.x

26. Pottosin I, Schönknecht G. Vacuolar calcium channels. J Exp Botany. 2007; 58:1559–1569. https://doi.org/10.1093/jxb/erm035

27. Carpaneto A, Canti A, Gambale F. Redox agents regulate ion channels activity in vacuoles from higher plant cells. FEBS Letters. 1999; 442:129–132. https://doi.org/10.1016/s0014-5793(98)01642-1 PMID: 9928987

28. Allen GJ, Sanders D. Vacuolar ion channels in higher plants. In: Leigh RA, Sanders D, editors. Advances in Botanical Research. Academic Press, London; 1997. p. 217–250.

29. Pantoja O, Gelli A, Blumwald E. Voltage-Dependent Calcium Channels in Plant Vacuole. Science. 1992; 255:1567–1570. https://doi.org/10.1126/science.255.5051.1567 PMID: 17820172

30. Trela Z, Burdach Z, Przestalski S, Karcz W. Effect of trimethyllead chloride on slowly activating (SV) channels in red beet (Beta vulgaris L.) taproots. Comptes Rendus Biologies. 2012; 335:722–730.

31. Neher E, Sakmann B. Single-channel currents recorded from membrane. Nature. 1976; 260:799–802. https://doi.org/10.1038/260799a0 PMID: 1083489

32. Hurst H. Long-term storage capacity of reservoirs. Trans Amer Soc Civil Eng. 1951; 116:770–808.

33. Bassingthwaighte JB, Raymond GM. Evaluating Rescaled Range Analysis for Time Series. Annals of Biomedical Engineering. 1994; 22:432–44. https://doi.org/10.1007/bf02368250 PMID: 7998689

34. Caccia DC, Percival D, Cannon MJ, Raymond G, Bassingthwaighte JB. Analyzing exact fractal time series: evaluating dispersional analysis and rescaled range methods. Physica A. 1997; 246(3-4):609–632. https://doi.org/10.1016/S0378-4371(97)00363-4 PMID: 22049251

35. Peng C, Buldyrev SV, Havlin S, Simons M, Stanley HE, Goldberger AL. Mosaic organization of DNA nucleotides. Physical Review E. 1994; 49(2):1685. https://doi.org/10.1103/PhysRevE.49.1685

36. Mercik S, Weron K. Stochastic origins of the long-range correlations of ionic current fluctuations in membrane channels. Physical Review. 2001; 63:1–10.

37. Mercik S, Weron K, Siwy Z. Statistical analysis of ionic current fluctuations in membrane channels. Physical Review E. 1999; 60(6):7343–7348. https://doi.org/10.1103/PhysRevE.60.7343

38. Lan Th, Gao Zy, Abdalla AN, Cheng B, Wang S. Detrended fluctuation analysis as a statistical method to study ion single channel signal. Cell Biology International. 2008; 32:247–252. https://doi.org/10.1016/j.cellbi.2007.09.001 PMID: 17964191

39. Siwy Z, Ausloos M, Ivanova K. Correlation studies of open and closed state fluctuations in an ion channel: Analysis of ion current through a large-conductance locust potassium channel. Phys Rev E. 2002; 65(3):31907. https://doi.org/10.1103/PhysRevE.65.031907

40. Weron R. Estimating long-range dependence: finite sample properties and confidence intervals. Physica A. 2002; 312(1-2):285–299. https://doi.org/10.1016/S0378-4371(02)00961-5

41. Mielniczuk J, Wojdyłło P. Estimation of Hurst exponent revisited. Computational Statistics & Data Analysis. 2007; 51:4510–4525. https://doi.org/10.1016/j.csda.2006.07.033

42. Bertl A, Blumwald E, Coronado R, Eisenberg R, Findlay G, Gradmann D, et al. Electrical measurements on endomembranes. Science. 1992; 258(5084):873–874.

43. Kepplinger KJF, Forstner G, Kahr H, Leitner K, Pammer P, Groschner K, et al. Molecular determinant for rundown of L-type Ca^{2+} channels localized in the carboxyl terminus of the α_{1C} subunit. Journal of Physiology 2000; 529(1): 119–130. https://doi.org/10.1111/j.1469-7793.2000.00119.x PMID: 11080256

44. Allen GJ, Sanders D. Calcineurin, a Type 2B Protein Phosphatase, Modulates the Ca2+-Permeable Slow Vacuolar Ion Channel of Stomatal Guard Cells. The Plant Cell 1995; 7(9):1473–1483. https://doi.org/10.1105/tpc.7.9.1473 PMID: 12242407

45. Gelli A, Blumwald E. Calcium Retrieval from Vacuolar Pools (Characterization of a Vacuolar Calcium Channel). Plant Physiology 1993; 102(4):1139–1146. https://doi.org/10.1104/pp.102.4.1139 PMID: 12231891

46. Ramanan SV, Valiunas V, Brink PR. Non-Stationary Fluctuation Analysis of Macroscopic Gap Junction Channel Records. Journal Membrane Biology 2005; 205(2):81–88. https://doi.org/10.1007/s00232-005-0765-4 PMID: 16283588

47. Lippiad J. Whole-cell recording using the perforated patch clamp technique. Methods in Molecular Biology 2008; 491:141–149. https://doi.org/10.1007/978-1-59745-526-8_11

48. Carpaneto A, Cantu AM, Gambale F. Redox agents regulate ion channel activity in vacuoles from higher plant cells FEBS Letters 1999; 442(2):129–132. https://doi.org/10.1016/s0014-5793(98)01642-1 PMID: 9928987

49. Sottocornola B, Visconti S, Orsi S, Gazzarrini S, Giacometti S, Olivari C, et al. The Potassium Channel KAT1 Is Activated by Plant and Animal 14-3-3 Proteins. Journal of Biological Chemistry. 2006; 281(47):35735–35741. https://doi.org/10.1074/jbc.M603361200 PMID: 16990282

50. Thomas SV, Kathpalia PP, Rajagopal M, Charlton C, Zhang J, Eaton DC, et al. Epithelial Sodium Channel Regulation by Cell Surface-associated Serum- and Glucocorticoid-regulated Kinase Journal of Biological Chemistry. 2011; 286(37):32074–32085. https://doi.org/10.1074/jbc.M111.278283 PMID: 21784856

51. Davison AC, Hinkley D. Bootstrap Methods and Their Application. New York: Cambridge University Press; 1997.

52. Miller FP, Vandome AF, McBrewster J. Kernel Density Estimation. Alphascript Publishing; 2010.

53. Silverman BW. Density estimation for statistics and data analysis. Monographs on statistics and applied probability. Chapman and Hall; 1986.

54. Peters EE. Fractal market analysis: applying chaos theory to investment and economics. Wiley Finance. J. Wiley & Sons; 1994.

55. Nait-Ali A. Advanced Biosignal Processing. Springer; 2009.

56. Palma W. Long-memory time series: theory and methods. Wiley series in probability and mathematical statistics. Probability and mathematical statistics. Wiley-Interscience; 2007.

57. Vandewalle N., Ausloos M., Boveroux Ph. Detrended fluctuation analysis of the foreign exchange market. Econophysic Workshop, Budapest, Hungary. 1997.

58. Wawrzkiewicz A, Pawelek K, Borys P, Dworakowska B, Grzywna ZJ. On the simple random-walk models of ion-channel gate dynamics reflecting long-term memory. European Biophysics Journal. 2012; 41(6):505–526. https://doi.org/10.1007/s00249-012-0806-8 PMID: 22484857

59. Berg HC. Random Walks in Biology. Princeton University Press; 1993.

60. Siwy Z, Mercik S, Weron K, Ausloos M. Application of dwell-time series in studies of long-range correlation in single channel ion transport: Analysis of ion current through a big conductance locust potassium channel. Physica A. 2001; 297:79–96. https://doi.org/10.1016/S0378-4371(01)00194-7